NASA TN D-249

TECHNICAL NOTE
D - 249

ANALYSIS OF LOW-ACCELERATION LIFTING ENTRY FROM ESCAPE SPEED

By Frederick C. Grant

Langley Research Center
Langley Field, Va.

NATIONAL AERONAUTICS AND SPACE ADMINISTRATION

WASHINGTON

June 1960

NATIONAL AERONAUTICS AND SPACE ADMINISTRATION

TECHNICAL NOTE D-249

ANALYSIS OF LOW-ACCELERATION LIFTING ENTRY FROM ESCAPE SPEED

By Frederick C. Grant

SUMMARY

An earlier analysis of lifting satellite entry for circular orbit velocities is extended to the case of parabolic orbit velocities. Simple formulas are derived which yield approximations to the minimum loadings for steep entries. The general advantage of operation on the high-drag side of maximum lift-drag ratio is demonstrated analytically. The optimum character of modulation from maximum lift coefficient is shown.

A principal parameter is shown to be the ratio of maximum lift coefficient to minimum drag coefficient. The analytical results are compared with those of detailed numerical integrations for an entry vehicle with a simplified but realistic lift polar.

INTRODUCTION

A lift program yielding low entry accelerations was proposed and analyzed by Lees, Hartwig, and Cohen in reference 1. In the program of reference 1, an initial period of constant resultant-force coefficient ($\dot{C}_R = 0$) is followed by one of constant resultant force ($\dot{R} = 0$) at the end of which the vehicle has essentially leveled out and the lift coefficient is zero. The simplified lift polar used in reference 1 is one for which the drag coefficient is constant. The analysis of reference 2, performed for circular velocities, shows that the use of realistic lift polars leads to greater reductions in peak loading than are indicated on the assumption of constant drag coefficient.

In reference 3, the variation of drag coefficient with lift coefficient is considered, but lift modulation is restricted to the direction of lower lift-drag L/D ratios for both the high- and low-drag sides of maximum L/D ratio. A physical argument of reference 2 indicates that modulation toward higher L/D ratios from maximum lift coefficient produces the lowest peak loadings.

In the present paper an analytical formulation of the general advantage of lift modulation on the high-drag side of maximum lift-drag ratio is given with a special application of the analysis to the case of entry from escape speed.

The analysis is limited by the assumptions of constant velocity during the modulated pullup and of an exponential variation of density with altitude. Although these assumptions can be refined, the unrefined results are satisfactory for estimation purposes. Numerical integration in a more exact atmosphere seems a logical second step if better results are required.

The scope of the analysis is restricted to the first pullup of the atmospheric entry. Problems associated with the remaining trajectory are not considered.

SYMBOLS

C_D	drag coefficient
C_L	lift coefficient
C_R	resultant-force coefficient
D	drag force
F	net acceleration due to gravity and centrifugal force
g	acceleration of gravity
H	altitude above sea level
I	acceleration parameter
L	lift force
m	mass
Q_s	total heat input
q_s	stagnation-point heating rate
R	resultant force, $\sqrt{L^2 + D^2}$
r	radial distance from earth's center

S	reference area
t	time
V	velocity
W	sea-level weight
β^{-1}	scale height, $-\frac{dH}{d \log_e \rho}$
Γ	minimum acceleration index
γ	flight-path angle, positive up
ρ	air density

Subscripts:

A	minimum drag
P	maximum lift
C	maximum lift-drag ratio
Q	maximum lift-drag ratio on optimum polar
B	point on polar intermediate to C and P
1	initial
2	final
n	nth approximation
max	maximum
min	minimum
pe	perigee distance
r	radial distance
o	sea level

A dot above a symbol indicates the derivative with respect to time.

ANALYSIS

The low-acceleration entry of references 1 and 2 may be divided into three phases as indicated in figure 1. These phases are treated separately as follows:

Approach Phase ($\rho = 0$)

For parabolic approach orbits, the variations with radial distance r of the velocity V and flight-path angle γ are

$$V^2 = 2rg_r \tag{1a}$$

$$r - r_{pe} = r \sin^2\gamma \tag{1b}$$

where r_{pe} is perigee distance and g_r is the local acceleration of gravity at radial distance r from the earth's center.

Constant-Loading Phase ($\dot{R} = 0$)

Passing over the $\dot{C}_R = 0$ phase of entry, consider the $\dot{R} = 0$ portion. As in reference 2, the aerodynamic coefficients are presumed to move from P to A on the lift polar (fig. 2) during the $\dot{R} = 0$ phase of entry. The following approximations are assumed in the analysis:

$$\gamma_A = 0$$

$$\rho = \rho_o e^{-\beta H}$$

$$\dot{V} = 0$$

$$\sin\gamma = \gamma$$

$$\cos\gamma = 1$$

The net radial acceleration F due to gravity and centrifugal force cannot be assumed to be zero as in the circular velocity entry of reference 2. In fact, for approach on a parabolic orbit $F = \frac{V^2}{r} - g_r$ has the value $F = g_r$. Since g_r does not vary appreciably in the atmosphere and since

the velocity is assumed to be constant, the approximation will be adopted that $F = g_o$. The lifting equation thus becomes

$$L + mg_o = mV\dot{\gamma} \tag{2}$$

Approximately 1 g unit of lifting acceleration is thus operative without any loading penalty. For constant velocity, the differential relation for a constant value of R is

$$\frac{dR}{R} = \frac{dC_R}{C_R} + \frac{d\rho}{\rho} = 0 \tag{3}$$

Introducing equation (3) into equation (2), with the additional substitutions $\dot{H} = V\gamma$ and $-\beta\, dH = \frac{d\rho}{\rho}$, yields after integration (ref. 2)

$$\frac{R_{AP}}{W} = \frac{\beta}{2g_o} \frac{V^2\gamma_P^2 - \frac{2g_o}{\beta} \log_e \frac{C_{R,P}}{C_{R,A}}}{I_{AP}} \tag{4a}$$

or

$$\frac{R_{AP}}{W} = \frac{\beta}{2g_o} \frac{V^2\gamma_P^2}{I_{AP}} - \frac{\log_e \frac{C_{R,P}}{C_{R,A}}}{I_{AP}} \tag{4b}$$

The third member of equation (4b) indicates the reduction in aerodynamic loading resulting from the extra g unit of lifting acceleration mentioned above. The acceleration parameter I_{AP} is an integral of the aerodynamic coefficients given by

$$I_{AP} = \int_A^P \frac{C_L}{C_R}\, d \log_e C_R \tag{5}$$

For a given lift polar I_{AP} can be readily evaluated graphically. (See ref. 2.)

Constant-Coefficient Phase ($\dot{C}_R = 0$)

The $C_R = 0$ phase is assumed, as in reference 2, to be flown at maximum lift coefficient $C_{L,P}$. Since the constant-coefficient phase separates the approach from the constant-loading phase (fig. 1), there is a boundary-value problem at each end. The problem is nontrivial only at the end beyond which $\dot{R} = 0$. Rewriting equation (2) with $g_o = \frac{V_1^2}{2r_1}$ and $\dot{\gamma} = V\gamma \frac{d\gamma}{dH}$ yields

$$C_{L,P} \frac{\rho}{2} SV_1^2 + m \frac{V_1^2}{2r_1} = mV_1^2\gamma \frac{d\gamma}{dH} \tag{6}$$

where C_L and V are constant. Integration of equation (6) with $\rho dH = -\frac{d\rho}{\beta}$ and $\rho_1 = 0$ yields

$$C_{L,P} \frac{S}{m} \rho_P + \frac{\beta(H_1 - H_P)}{r_1} = \beta\gamma_1^2 - \beta\gamma_P^2 \tag{7}$$

Rewriting equation (4) with $g_o = \frac{V_1^2}{2r_1}$ and $\frac{1}{\beta} \log_e \frac{C_{R,P}}{C_{R,A}} = H_P - H_A$ yields

$$I_{AP}C_{R,P} \frac{S}{m} \rho_P + \frac{\beta(H_P - H_A)}{r_1} = \beta\gamma_P^2 \tag{8}$$

Adding equations (7) and (8), solving for ρ_P, and substituting $\rho_P = \frac{C_{R,A}}{C_{R,P}} \rho_A$ yields

$$\rho_A = \frac{\beta}{g_o} \frac{\gamma_1^2 - \frac{H_1 - H_A}{r_1}}{\frac{C_{R,A}S}{W}\left(\frac{C_{L,P}}{C_{R,P}} + I_{AP}\right)} \tag{9}$$

for the density at the minimum altitude in terms of intial conditions. Multiplying equation (9) by $C_{R,A} \frac{S}{W} \frac{V_1^2}{2}$ yields the peak acceleration in terms of intial conditions as

$$\frac{R_{AP}}{W} = \frac{\frac{\beta}{2g_o} V_1^2 \gamma_1^2 - \beta(H_1 - H_A)}{\frac{C_{L,P}}{C_{R,P}} + I_{AP}} \tag{10}$$

Equation (9) is transcendental in the minimum altitude H_A. It may be readily solved by iteration. If the term due to F, which is $\frac{H_1 - H_A}{r_1}$, is assumed to be zero, a first value of H_A is obtained as

$$\beta(H_A)_1 = \log_e \rho_o - \log_e \frac{\beta}{g_o} \frac{\gamma_1^2}{\frac{C_{R,A} S}{W}\left(\frac{C_{L,P}}{C_{R,P}} + I_{AP}\right)} \tag{11a}$$

A second approximation is found with the relation

$$\beta\left[(H_A)_2 - (H_A)_1\right] = -\log_e\left[1 - \frac{H_1 - (H_A)_1}{r_1 \gamma_1^2}\right] \tag{11b}$$

In the general case, the following relation will converge on H_A:

$$\beta\left[(H_A)_{(n+2)} - (H_A)_{(n+1)}\right] = -\log_e\left[\frac{1 - \frac{H_1 - (H_A)_{(n+1)}}{\gamma_1^2 r_1}}{1 - \frac{H_1 - (H_A)_n}{\gamma_1^2 r_1}}\right] \tag{11c}$$

With the value of H_A established, the conditions at point P are readily calculated. The entry is thus defined as far as the minimum altitude H_A. For polar AQP which gives I_{AP} a maximum value (ref. 2) equation (10) becomes

$$\frac{R_{AQP}}{W} = \frac{\frac{\beta}{2g_o} V_1^2 \gamma_1^2 - \beta(H_1 - H_A)}{\sinh^{-1} \frac{C_{L,P}}{C_{R,A}}} \tag{12}$$

The denominator of the right side of equation (12), which defines an upper bound to the possible acceleration reduction, is plotted in figure 3. The most rapid increase in the value of the function occurs at the lower end of the range; this indicates in a rough way that large gains in maximum L/D ratio (low values of $C_{R,A}$) do not lead to corresponding large reductions in peak loading after a certain amount of reduction has already been achieved. Formula (12) and figure 3 allow a quick estimate of the minimum loading in terms of the maximum lift and minimum drag coefficients. A corresponding quick estimate of H_A is obtained in equation (11a) by the same substitution

$$\beta(H_A)_1 = \log_e \rho_o - \log_e \frac{\beta}{g_o} \frac{\gamma_1^2}{\frac{C_{R,A}S}{W} \sinh^{-1} \frac{C_{L,P}}{C_{R,A}}} \tag{13}$$

Optimum Range of Modulation

For an entry pullup to $\gamma = 0$ with an $\dot{R} = 0$ modulation phase bounded by arbitrary points 1 and 2 on the lift polar, the analog to equation (10) indicates that

$$\frac{R}{W} \propto \frac{1}{\Gamma}$$

where

$$\Gamma = \left(\frac{C_L}{C_R}\right)_1 + \int_2^1 \frac{C_L}{C_R} \, d \log_e C_R \tag{14}$$

The integral term of equation (14) measures the contribution of the modulation. If point 2 is considered fixed, the change in Γ due to a change of the initial point on the polar is

$$d\Gamma = \left(\frac{dC_L}{C_R}\right)_1 \tag{15}$$

Thus, the maximum value of Γ occurs for $C_{R,1} = C_{R,P}$. If variations in point 2 are now admitted, the absolute maximum occurs for $C_{R,2} = C_{R,A}$. It is clear that if a lower limit exists on the lift coefficient to which the modulation can be carried, the best range of modulation lies between the minimum allowable and the maximum available lift coefficients.

For the class of unmodulated entries $C_{R,2} = C_{R,1}$. For these cases

$$d\Gamma = d\left(\frac{C_L}{C_R}\right)_1 \tag{16}$$

which yields the result that minimum R/W (maximum Γ) occurs for maximum L/D ratio. For the peak accelerations to be equal in a constant coefficient, maximum L/D ratio entry, and an entry from maximum lift coefficient with modulation the condition

$$\left(\frac{C_L}{C_R}\right)_C - \left(\frac{C_L}{C_R}\right)_P = \int_B^P \frac{C_L}{C_R}\, d \log_e C_R \tag{17}$$

must hold where B marks the minimum to which the coefficients must be reduced from P. For example, in the case of the lift polar of figure 2, $C_{L,B} = 0.45$. This example shows how the acceleration peak corresponding to an unmodulated entry at maximum L/D ratio can be matched on the high-drag side of maximum L/D ratio. Moreover, the quantity

$$\int_C^B \frac{C_L}{C_R}\, d \log_e C_R$$

is the increment in Γ which the modulated entry from $C_{L,P}$ enjoys when compared with modulated entry from maximum L/D ratio.

Relative Importance of Lift Modulation and Drag Modulation

It was indicated in reference 2 that the most desirable polar from the standpoint of loading reduction was the right angle AQP shown in figure 4. For this polar, the quantity Γ has the value $\sinh^{-1} \frac{C_{L,P}}{C_{R,A}}$.

If the contributions to the value of Γ of the legs AQ and QP are considered separately, the secondary influence of changes in drag coefficient may be demonstrated. For the polar AQP

$$\Gamma_{AQP} = \frac{C_{L,P}}{C_{R,P}} + I_{AQP} = \frac{C_{L,P}}{C_{R,P}} + I_{AQ} + I_{QP} = \sinh^{-1} \frac{C_{L,P}}{C_{R,A}} \tag{18}$$

The contribution of the leg AQ along which there is lift modulation but no drag modulation may be written

$$I_{AQ} = \sinh^{-1}\left(\frac{C_{L,P}}{C_{R,A}}\right) - \frac{C_{L,Q}}{C_{R,Q}} \tag{19}$$

For leg QP along which there is drag modulation but no lift modulation,

$$I_{QP} = \frac{C_{L,Q}}{C_{R,Q}} - \frac{C_{L,P}}{C_{R,P}} \tag{20}$$

On summing up for Γ_{AQP}, the contribution of leg QP cancels out against the $C_{L,P}/C_{R,P}$ term of equation (18) and the third member of equation (19). Higher values of $C_{D,P}$ are thus exactly offset by resultant lower values of $C_{L,P}/C_{R,P}$. For polars which are less than ideal, the influence of changes in drag coefficient with lift coefficient results in reduced values of Γ for the same ratios of maximum lift to minimum drag coefficients.

In terms of the present analysis, the increase in drag coefficient with lift coefficient is a price that must be paid for higher lift coefficients. When maximum lift coefficient is reached, there are no further gains. If the idealization of constant velocity is dropped in the analysis, the value of the drag force is found in the fact that higher lift coefficients can be used at the same altitudes with the same loading limits. The dominant position of lift coefficient is unchanged.

Limiting Cases

Some limiting results can be derived in terms of the optimum polar AQP of figure 4. If unmodulated entry from escape speed at maximum L/D ratio is considered as $L/D \to \infty$ $(C_{R,A} \to 0)$, the limiting value of the peak loading is found to be

$$\frac{R}{W} = \frac{\beta}{2g_o} V_1^2 \gamma_1^2 - \beta(H_1 - H_A) \tag{21}$$

If modulation is now admitted and again the maximum L/D ratio becomes infinite, the limit loading is found to be

$$\frac{R}{W} = 0 \tag{22}$$

The different results in the two cases can be explained in terms of the pullout altitude H_A. In the unmodulated case, a finite lift coefficient for the entry implies a finite loading and finite pullout altitude. In the modulated case, a zero lift coefficient implies an infinite depth of penetration of the atmosphere to complete the pullup. The vanishing of $C_{R,A}$ allows indefinite penetration without a loading penalty when modulation is used.

RESULTS

Parameters and Initial Conditions

All results are for a vehicle with the idealized drag polar of figure 2. The aerodynamic characteristics and wing loading are as follows:

$C_{R,A} = 0.025$ $\qquad (L/D)_C = 2.8$

$C_{L,P} = 0.75$

$C_{D,P} = 0.75$ $\qquad W/S = 25$ lb/sq ft

The value of β^{-1} used for the approximate analysis was based on the densities at 10^5 and 3×10^5 feet of altitude in the ARDC atmosphere

(ref. 4). This value of β^{-1} is 23,300 feet. The initial conditions considered were as follows:

$$H_1 = 350{,}000 \text{ ft}$$

$$V_1 = 36{,}500 \text{ ft/sec}$$

Numerical Values

Detailed numerical integrations of entry into the ARDC atmosphere are compared with the analytic results for given values of γ_1 and $(R/W)_{max}$ in the following table (V_1 = 36,500 ft/sec and H_1 = 350,000 feet):

	$-\gamma_1 = 12^\circ$		$(R/W)_{max} = 10$	
	Analytical	Numerical (a)	Analytical	Numerical (b)
$(R/W)_{max}$ . . .	7.6	6.30	10	10
$-\gamma_1$, deg . . .	12	12	13.4	14.7
H_A, ft	1.24×10^5	1.26×10^5	1.17×10^5	1.11×10^5
$-\gamma_A$, deg . . .	0	0.51	0	0.71
V_A	V_1	$0.88V_1$	V_1	$0.85V_1$
$C_{R,A}$	0.025	0.0276	0.025	0.0273
$C_{L,A}$	0	0.0113	0	0.0106
$C_{D,A}$	0.025	0.0252	0.025	0.0251
H_P, ft	2.11×10^5	2.25×10^5	2.05×10^5	2.14×10^5
$-\gamma_P$, deg . . .	11.0	10.4	12.3	12.9
V_P	V_1	$0.99V_1$	V_1	$0.99V_1$

[a]The values shown as occurring at A actually occur at the minimum coefficient attained with $(R/W)_{max} = 6.30$. Other numerical results show the minimum value of $(R/W)_{max}$ to be greater than 6.25.

[b]As in the case of $-\gamma_1 = 12^\circ$, the values quoted for A occur at the minimum coefficients attained. Other results show that for $-\gamma_1 = 14.8^\circ$, $(R/W)_{max} > 10$.

For $-\gamma_1 = 12^\circ$, the analysis indicates a value of $(R/W)_{max}$ about 20 percent higher than that actually possible. This difference is the combined result of the 12 percent loss of speed during the entry and the variation of β with altitude. Since the assumptions of the analysis lead to conservative results, use of the nonconservative equation (12) and figure 3 gives better agreement with the numerical integrations. For entry conditions corresponding to those given in the table, reference 1 indicates a minimum $(R/W)_{max}$ of about 11.5 for $-\gamma_1 = 12^\circ$.

For the given load limit, $(R/W)_{max} = 10$, an outstanding favorable feature of the table is the steep entry angle, nearly 15°, which corresponds to a $10g_o$ limit with modulation to zero lift. Strikingly unfavorable is the low value of minimum altitude H_A, just over 100,000 feet, corresponding to maximum lift modulation at a $10g_o$ load limit.

Entry Corridor

For a given load limit, $(R/W)_{max} = 10$, the numerical and analytic results are compared in terms of entry corridor width in figure 5. The $\dot{C}_D = 0$, $\dot{C}_L \neq 0$ curve, though taken from reference 3, is based on the results of reference 1. The overshoot limit of the present analysis is taken as the altitude at which the maximum lift coefficient in inverted flight will produce a component of acceleration equal to g_o at parabolic orbit speed. Only single points are shown for the present analysis representing entry from the favorable initial value, $C_{L,1} = C_{L,P}$ (fig. 2). For decreasing values of $C_{R,1} < C_{R,P}$, the points move toward the $\dot{C}_D = 0$, $\dot{C}_L \neq 0$ curve as indicated by the arrows. Calculations for a family of vehicles with different polars and different maximum lift-drag ratios would result in a curve such as those shown from reference 3. Without a functional relation between Γ and $(L/D)_{max}$ the present analysis will not yield a generalized curve.

It is evident from figure 5 that large gains in corridor width appear if a realistic lift polar is used. Whether these gains can be realized depends on the severity of the heating problem accompanying steep entries. In any case, the heating problem is less severe for modulation from maximum lift coefficient ($\dot{C}_D$, $\dot{C}_L \neq 0$ in fig. 5) than for modulation from maximum lift-drag ratio ($\dot{C}_D = 0$, $\dot{C}_L \neq 0$ in fig. 5).

Heating

Some indication of the conflict to be resolved between low heating and low accelerations is given in figure 6 for entries at escape speed

with modulation from maximum lift coefficient. An approximate value of laminar stagnation heating rate is (ref. 5)

$$q_s = 17{,}300\sqrt{\rho}\left(\frac{V}{10^4}\right)^{3.15} \frac{\text{Btu}}{\text{ft}^2\text{-sec}} \qquad (23)$$

where ρ is in slugs per cubic feet and V is in feet per second. Formula (23) is applicable to 1-foot-radius spheres in the neighborhood of satellite speed. Although use of formula (23) may not be justified at escape speed, it offers a convenient measure of the relative heating problems on different trajectories.

The integral of q_s with respect to time through the bottom of the pullup yields a measure of the total heat input Q_s at stagnation-point conditions. If this heat input is absorbed by ablation, Q_s is also a measure of the amount of ablative material consumed in the pullup.

Values of Q_s are shown in figure 6 along with the minimum lift coefficients to which modulation was carried for a $10g_o$ load limit. The figure shows the highest attainable entry angles for a $10g_o$ load limit if the minimum lift coefficients attained are regarded as the lowest allowable values. There is a rapid rise in Q_s at the lowest values of minimum lift coefficient which correspond to full use of the load-reduction potential of the vehicle. For a minimum lift coefficient of zero, the heat load is 5.5 times that experienced during a pullup at maximum lift coefficient. However, by reduction of the entry angle (corridor width) large corridor widths can still be maintained with lower heat loads. For example, if the minimum lift coefficient is taken as 0.2 instead of zero, Q_s is 2.1 times the value corresponding to entry at maximum lift coefficient. The corridor width becomes 220 kilometers instead of 387 kilometers, but both widths are large.

The strong coupling shown in figure 6 between heat load and entry angle (corridor width) suggests that guidance capability must be considered if the conflict between heating penalty and corridor width is to be resolved. Obviously, heating and acceleration considerations alone are insufficient for vehicles with large lift modulation capability.

CONCLUDING REMARKS

For steep entry from satellite or escape speed, maximum lift coefficient is established analytically as the point from which the lift should be modulated for the greatest loading reduction. In place of maximum lift-drag ratio as an index of potential acceleration reduction for

unmodulated entries, the present analysis has a logarithmic function of the ratio of maximum lift coefficient to minimum drag coefficient. The analysis illustrates the leading position of lift-coefficient variation as compared with drag-coefficient variation in the reduction of peak loadings through angle-of-attack reduction.

Langley Research Center,
National Aeronautics and Space Administration,
Langley Field, Va., January 6, 1960.

REFERENCES

1. Lees, Lester, Hartwig, Frederic W., and Cohen, Clarence B.: The Use of Aerodynamic Lift During Entry Into the Earth's Atmosphere. GM-TR-0165-00519, Space Tech. Labs., Inc., Nov. 20, 1958.

2. Grant, Frederick C.: Importance of the Variation of Drag With Lift in Minimization of Satellite Entry Acceleration. NASA TN D-120, 1959.

3. Chapman, Dean R.: An Analysis of the Corridor and Guidance Requirements for Supercircular Entry Into Planetary Atmospheres. NASA TR R-55, 1960.

4. Minzner, R. A., and Ripley, W. S.: The ARDC Model Atmosphere, 1956. Air Force Surveys in Geophysics No. 86 (AFCRC TN-56-204, ASTIA Doc. 110233), Air Force Cambridge Res. Center, Dec. 1956.

5. Chapman, Dean R.: An Approximate Analytical Method for Studying Entry Into Planetary Atmospheres. NASA TR R-11, 1959. (Supersedes NACA TN 4276.)

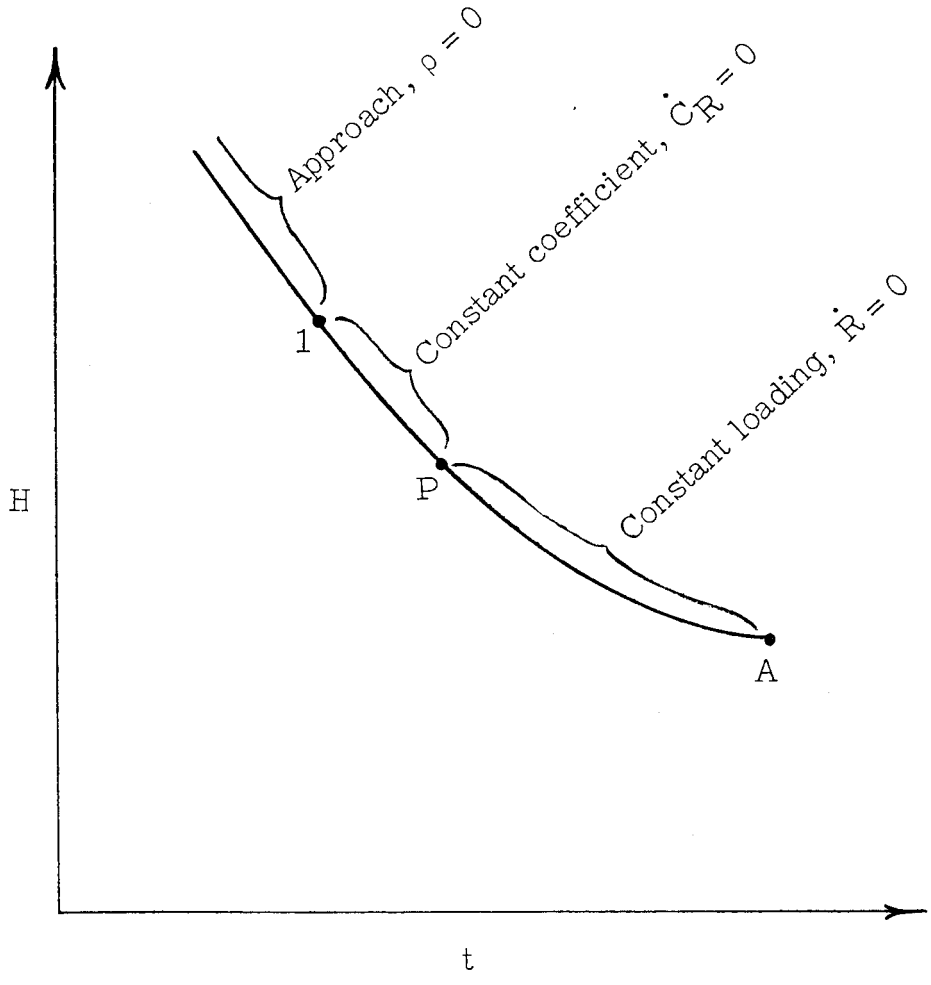

Figure 1.- Three phases of entry considered in analysis.

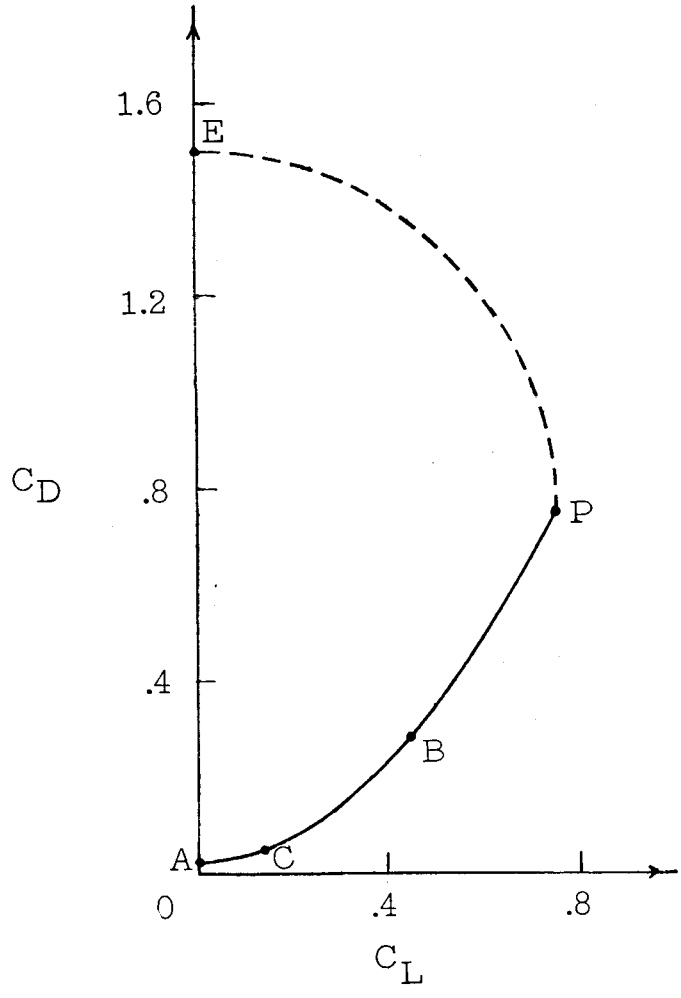

Figure 2.- Idealized lift polar for an entry vehicle.

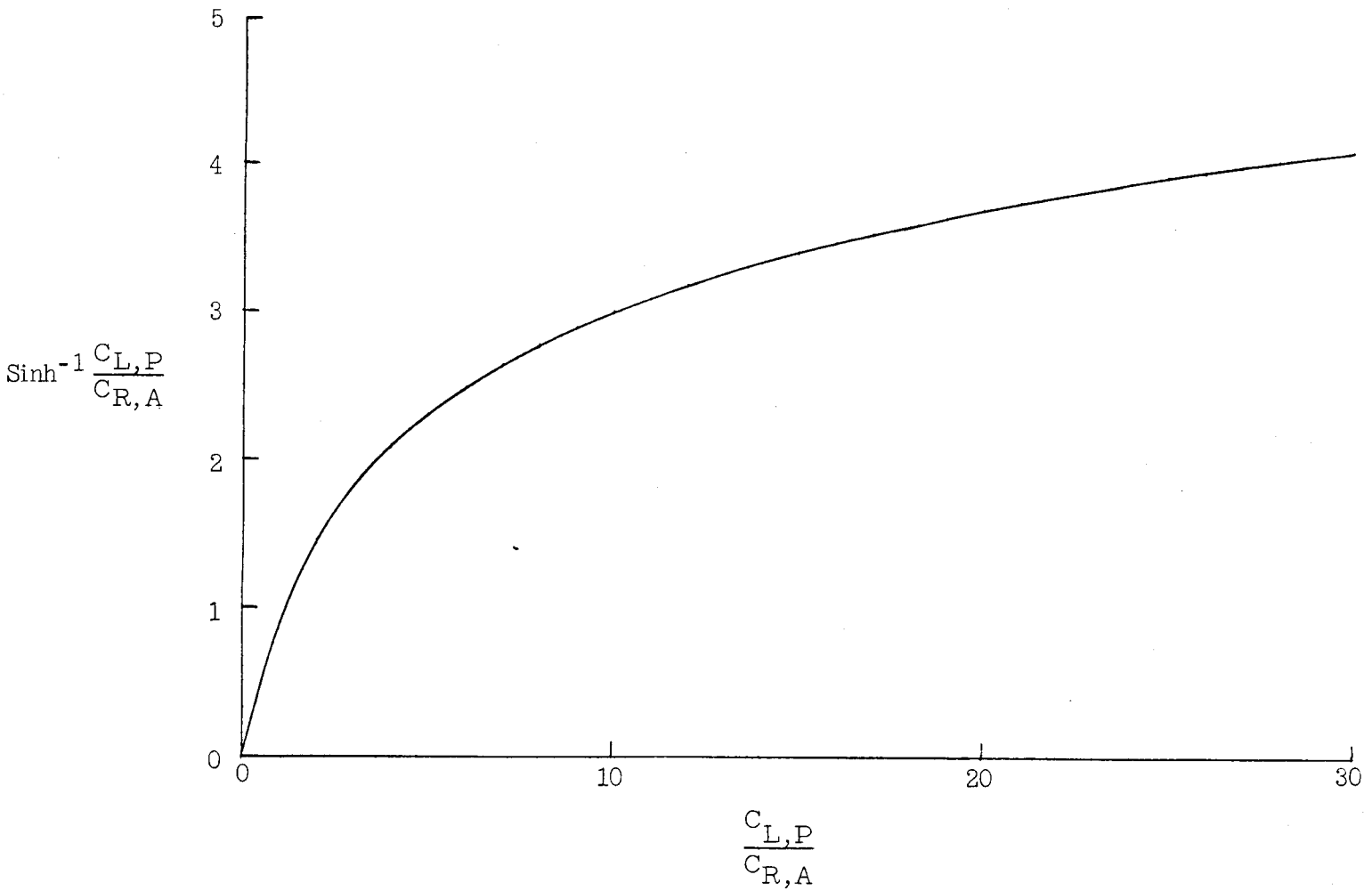

Figure 3.- Function to which minimum value of $(R/W)_{max}$ is inversely proportional.

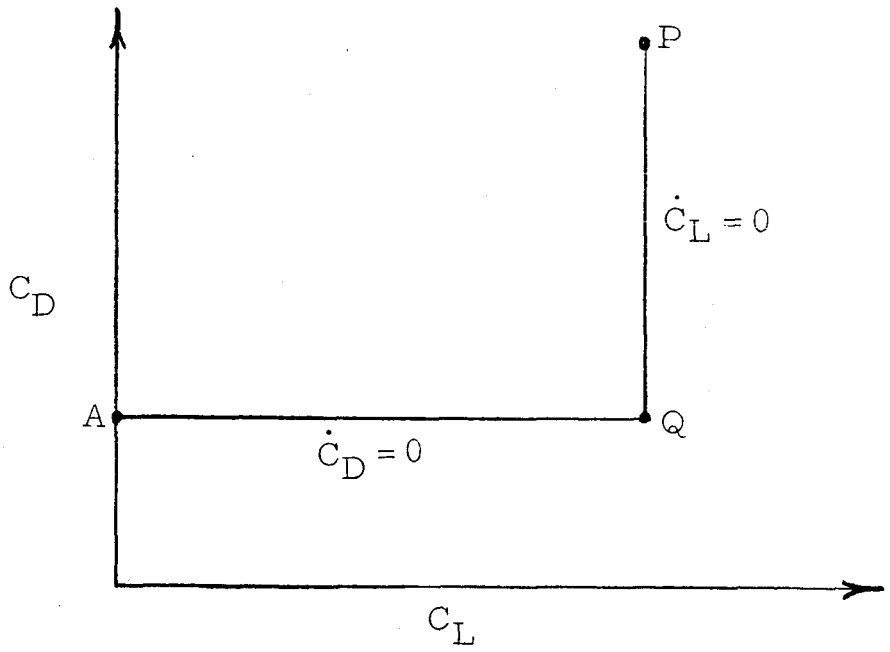

Figure 4.- Polar yielding maximum loading reduction.

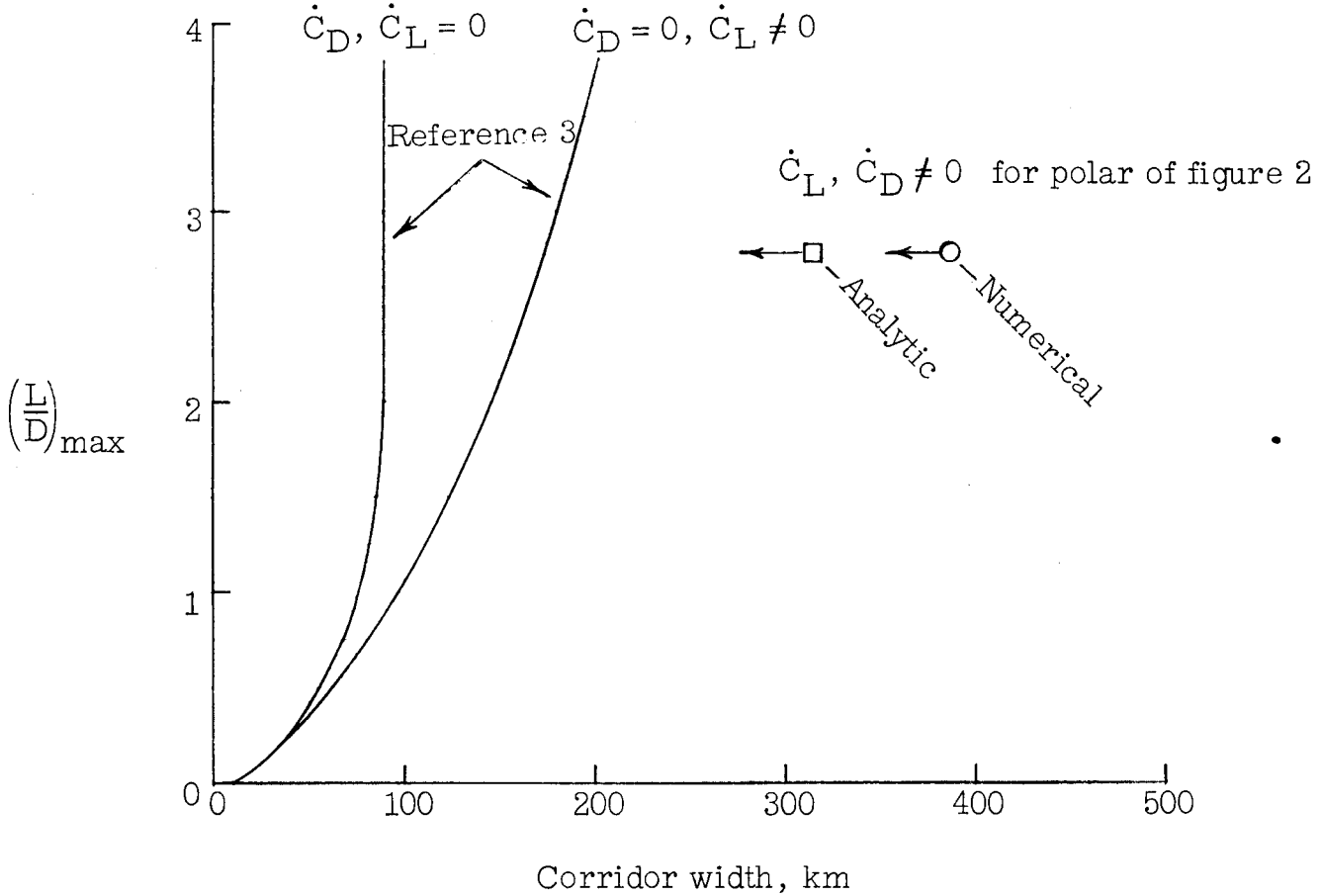

Figure 5.- Entry corridor widths for parabolic approach orbits. $(R/W)_{max} = 10$.

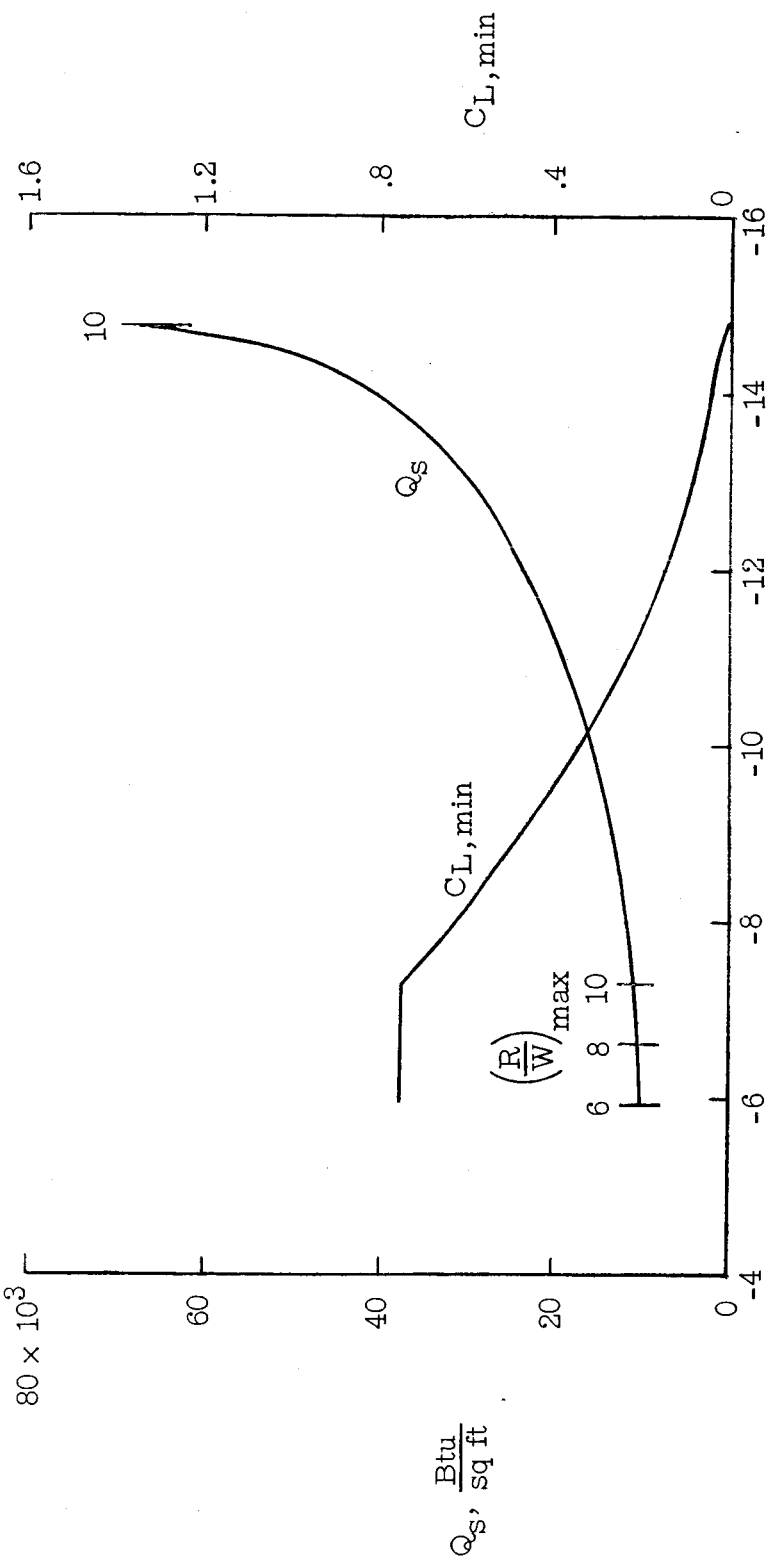

Figure 6.- Variation of total heat and minimum lift coefficient with entry angle. $(R/W)_{max} \leq 10$.